

A Fluorescent Probe for Imaging Sirtuin Activity in Living Cells, Based on One-Step Cleavage of the Dabcyl Quencher

Mitsuyasu Kawaguchi, Shohei Ikegawa, Naoya Ieda, and Hidehiko Nakagawa^{*[a]}

Sirtuins (SIRT) are a family of NAD⁺-dependent histone deacetylases. In mammals, dysfunction of SIRT is associated with age-related metabolic diseases and cancers, so SIRT modulators are considered attractive therapeutic targets. However, current screening methodologies are problematic, and no tools for imaging endogenous SIRT activity in living cells have been available until now. In this work we present a series of simple and highly sensitive new SIRT activity probes. Fluorescence of these probes is activated by SIRT-mediated hydrolytic release of a 4-(4-dimethylaminophenylazo)benzoyl (Dabcyl)-

based FRET quencher moiety from the ϵ -amino group of lysine in a nonapeptide derived from histone H3K9 and bearing a C-terminal fluorophore. The probe SFP3 detected activities of SIRT1, -2, -3, and -6, which exhibit deacylase activities towards long-chain fatty acyl groups. We then truncated the molecular structure of SFP3 in order to improve both its stability to peptidases and its membrane permeability, and developed probe KST-F, which showed specificity for SIRT1 over SIRT2 and SIRT3. We show that KST-F can visualize endogenous SIRT1 activity in living cells.

Introduction

Sirtuins (SIRT), mammalian orthologues of yeast Sir2, are a family of NAD⁺-dependent histone deacetylases, their activities closely correlated with cellular energy levels.^[1] SIRT are involved in metabolic regulation, stabilization of genomic DNA, stress responses, and even aging,^[2] and SIRT modulators are considered attractive therapeutic targets.^[3]

Several methodologies to detect SIRT activity are available; they include the use of radioisotopes,^[4] antibodies,^[5] and HPLC.^[6] Fluorescent probes have also been widely used, due to their high sensitivity and commercial availability,^[7] but they generally require trypsin digestion of a C-terminal lysine residue in order to produce a fluorescence signal after the SIRT reaction.^[7] This requirement is problematic for screening purposes (e.g., trypsin inhibitors generate false-positive signals), and also makes it impossible to visualize SIRT activity in living cells with these probes. Therefore, a one-step procedure for detection of SIRT activity is desired, and one approach has indeed been reported by Kikuchi and co-workers.^[8] They utilized an intramolecular transesterification mechanism, which affords a fluorescence increase after deacetylation of a lysine residue by SIRT1. However, they found that the background fluorescence

gradually increases under aqueous conditions even in the absence of SIRT1, probably due to instability of the probe, which contains a carbonate group. Therefore, their probe might be restricted to enzymes with high activity, such as SIRT1 among the SIRT family, and it is unsuitable for cellular SIRT imaging. There is still a need for a stable, one-step fluorescence probe suitable for imaging SIRT activity in living cells.

For a long time, it was thought that SIRT catalyze deacetylation reactions of histones and that some SIRTs also catalyze ADP ribosylation.^[9] However, it is now known that some SIRTs show weak deacetylase activity, but have relatively strong deacylase activities instead: SIRT4, for example, shows lipoamidase activity,^[10] SIRT5 shows desuccinylase and demalonylase activities,^[11] and SIRT6 shows demyristoylase activity.^[12] The demyristoylase activity of SIRT6 regulates secretion of TNF- α .^[12] Interestingly, the X-ray crystal structure of SIRT6 shows a large hydrophobic pocket that accommodates the myristoyl group.^[12] Moreover, other reports indicate that several SIRTs, including SIRT1, -2, and -3, show deacylase activity towards lysine residues bearing long-chain fatty acyl groups, in addition to their strong deacetylase activities.^[13] These results suggest that SIRT1, -2, and -3 might also have large hydrophobic pockets for recognition of long-chain fatty acyl groups.^[14]

In this study we report new one-step SIRT activity probes that utilize this deacylase activity. Specifically, we hypothesized that lysine residues bearing large quencher dyes, such as 4-(4-dimethylaminophenylazo)benzoyl (Dabcyl) derivatives, would be recognized and hydrolyzed by SIRTs that have large hydrophobic pockets. On the basis of this hypothesis, we synthesized FRET-based SIRT probes SFP1–3 (Scheme 1, below), each containing a Dabcyl-based quencher, anticipating that their fluorescence would be activated by SIRT-mediated hydrolytic

[a] Dr. M. Kawaguchi, S. Ikegawa, Dr. N. Ieda, Prof. Dr. H. Nakagawa
Graduate School of Pharmaceutical Sciences, Nagoya City University
3-1 Tanabe-dori, Mizuho-ku, Nagoya, Aichi 467-8603 (Japan)
E-mail: deco@phar.nagoya-cu.ac.jp

Supporting information for this article can be found under <http://dx.doi.org/10.1002/cbic.201600374>.

© 2016 The Authors. Published by Wiley-VCH Verlag GmbH & Co. KGaA. This is an open access article under the terms of the Creative Commons Attribution-NonCommercial License, which permits use, distribution and reproduction in any medium, provided the original work is properly cited and is not used for commercial purposes.

release of the DabcyI moiety. Surprisingly, SFP3 was hydrolyzed by SIRT1, -2, -3, and -6, and was an excellent substrate for SIRT1 ($K_m = 0.10 \mu\text{M}$), with the release of DabcyI dyes. We then truncated the molecular structure of SFP3 to improve its stability and membrane permeability, obtaining probe KST-F. We show that KST-F can visualize endogenous SIRT1 activity in living cells. Recently, Schutkowski and co-workers reported a simple methodology for detecting SIRT activity in which long-chain acyl groups bearing small quencher moieties—2-amino-benzoylamide groups—at the other end of the chain are directly cleaved by SIRT2.^[15] We believe the discovery that DabcyI lysine is a SIRT substrate further expands the substrate scope of SIRTs and that the longer excitation wavelengths of DabcyI dyes should also be advantageous for activity measurements.

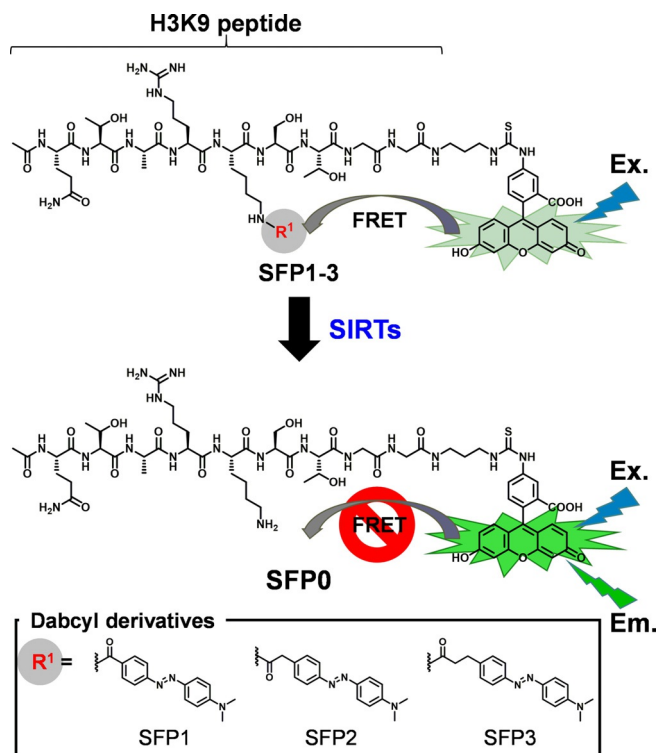
Results and Discussion

Strategy and molecular design for SIRT activity detection

As mentioned above, X-ray crystal structure analysis has revealed the presence of a large hydrophobic pocket in SIRT2 and also in SIRT2,^[12,14] and despite the absence of direct evidence, we speculated that SIRT1 and SIRT3 might have similar pockets. Therefore, taking into account that some SIRTs exhibit deacylase activities towards long-chain fatty acyl groups,^[12–14] we considered that the substrate-recognition pockets of SIRTs might be very flexible, and might recognize even DabcyI-based quencher moieties. On the basis of this hypothesis, we designed probes SFP1–3, each consisting of a nonapeptide derived from histone H3K9,^[16] a C-terminal fluorophore, and a DabcyI quencher dye attached to a lysine ϵ -amino group. In this design, we considered that the DabcyI moiety would quench the fluorescence of the fluorophore, but would be recognized and hydrolyzed by SIRTs with large hydrophobic pockets, resulting in a fluorescence increase, as shown in Scheme 1.

Synthesis and photochemical characteristics of SFP0–3

SFP1–3 were synthesized as shown in Schemes S1–3 in the Supporting Information. In brief, H3K9 nonapeptide was synthesized by means of Fmoc solid-phase synthesis on 2-chlorotrityl chloride resin. It was cleaved from the resin with weak acid (1% TFA) without cleavage of the protecting groups of the peptide sequence. The Cbz group on the lysine residue was removed, and three DabcyI derivatives (DabcyI, –EH and –PH) activated with succinimidyl ester moieties were linked to the ϵ -amino group. Fluorescein isothiocyanate (FITC)-DA-NH₂-TFA was attached at the C terminus of each peptide with (1-cyano-2-ethoxy-2-oxoethylideneaminoxy)dimethylamino-morpholinocarbenium hexafluorophosphate (COMU), and the protecting groups of FITC and the peptides were removed with K₂CO₃ and TFA, respectively. Each probe was purified by HPLC, and the structures were confirmed by HRMS. Using the same procedure, we also synthesized SFP0 (with a primary amine at the lysine residue) as the putative product of enzymatic reaction with SIRTs (Scheme S4).



Scheme 1. Schematic illustration of our strategy for one-step detection of SIRT activity.

We first measured the absorption and fluorescence spectra of SFP0–3 and calculated the fluorescence quantum yields (Figure 1, Table 1). SFP0 showed strong fluorescence ($\Phi_{\text{FL}} = 0.70$), whereas SFP1–3 showed very weak fluorescence, thus suggesting that FRET does occur in these molecules and effectively quenches the fluorescence of SFP1–3 ($\Phi_{\text{FL}} = 0.009$ – 0.031).

Enzymatic reactions and kinetics of SFP1–3 with SIRT6

We examined the reactions between SFP1–3 and SIRT6, the deacetylation activity of which is poor.^[12] Interestingly, fluorescence increments of SFP2 and SFP3, but not SFP1, were observed with SIRT6 (Figures 2A and S1). These fluorescence increments were SIRT6- and NAD⁺-dependent, and they were suppressed by nicotinamide (NAM), a pan-SIRT inhibitor,^[17] thus showing that they reflect SIRT6 enzymatic activity. The increase in fluorescence was higher with SFP3. This result suggests that SIRT6 shows a preference for aliphatic carboxylates (as in SFP2 and SFP3), in accordance with reports that SIRTs deacylate fatty acids, but not aromatic carboxylates.^[13] We next conducted a product analysis of the enzymatic reaction by HPLC (Figure 2B). The peak of SFP3 decreased time-dependently, and two new peaks were generated. We assigned these two peaks as SFP0 and DabcyI-PH. Thus, the enzymatic reaction between SFP3 and SIRT6 proceeded as we had expected, and the fluorescence increment was due to generation of SFP0. We also investigated the kinetics of the SIRT6 reaction. The K_m and k_{cat} values were found to be $2.1 \mu\text{M}$ and 0.0029 s^{-1} ,

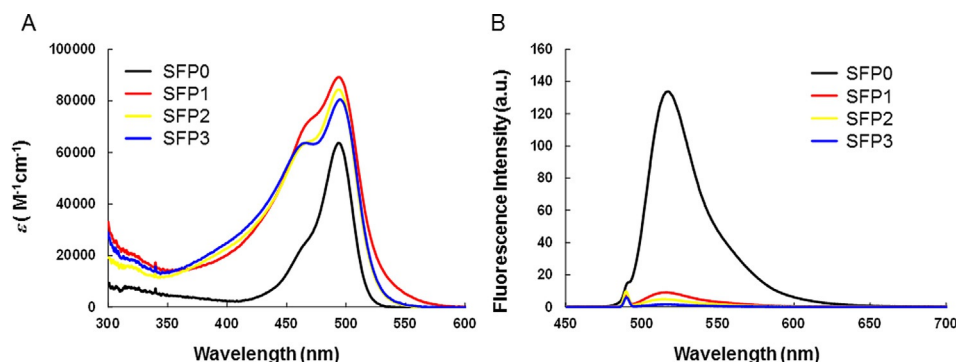


Figure 1. Absorption and fluorescence spectra of 2.5 μM SFP0, -1, -2, and -3. $\lambda_{\text{ex}} = 490$ nm. Measurements were made in sodium phosphate buffer (pH 7.4).

	λ_{max} [nm]	ϵ [$10^4 \text{ M}^{-1} \text{ cm}^{-1}$]	λ_{em} [nm]	Φ_{FL}
SFP0	494	6.37	516	0.700
SFP1	494	8.92	516	0.031
SFP2	494	8.44	517	0.015
SFP3	495	8.05	517	0.009

[a] Data were measured in sodium phosphate buffer (pH 7.4). For determination of Φ_{FL} , fluorescein in 0.1 N NaOH ($\Phi_{\text{FL}} = 0.85$) was used as a fluorescence standard.

SFP3	k_{cat} [s^{-1}]	K_{m} [μM]	$k_{\text{cat}}/K_{\text{m}}$ [$\text{s}^{-1} \text{ M}^{-1}$]	$K_{\text{m,NAD}}$ [μM]
SIRT1	0.023 ± 0.0086	0.10 ± 0.014	2.3×10^5	3.0
SIRT2	0.0024 ± 0.00008	0.52 ± 0.059	4.6×10^3	30
SIRT3	0.0019 ± 0.00003	7.7 ± 0.21	2.5×10^2	400
SIRT4	n.d.	n.d.	n.d.	n.d.
SIRT6	0.0029 ± 0.00009	2.1 ± 0.19	1.4×10^3	99

[a] For the determination of kinetic parameters, we used the following concentrations of SIRT5: 7 nM SIRT1, 24 nM SIRT2, 60 nM SIRT3, 32 nM SIRT4, and 48 nM SIRT6 (final conc.). n.d.: not determined (enzymatic reaction with SIRT4 was too slow to allow the values to be determined). For details, see the Supporting Information.

respectively (Figure 2C, Table 2). These values are similar to the reported values of H3K9 myristoyl and palmitoyl (C_{14} and C_{16}) derivatives,^[11] the K_{m} and k_{cat} values of which were $3.4 \mu\text{M}$ / 0.0049 s^{-1} , and $0.9 \mu\text{M}/0.0027 \text{ s}^{-1}$, respectively (Table S1).

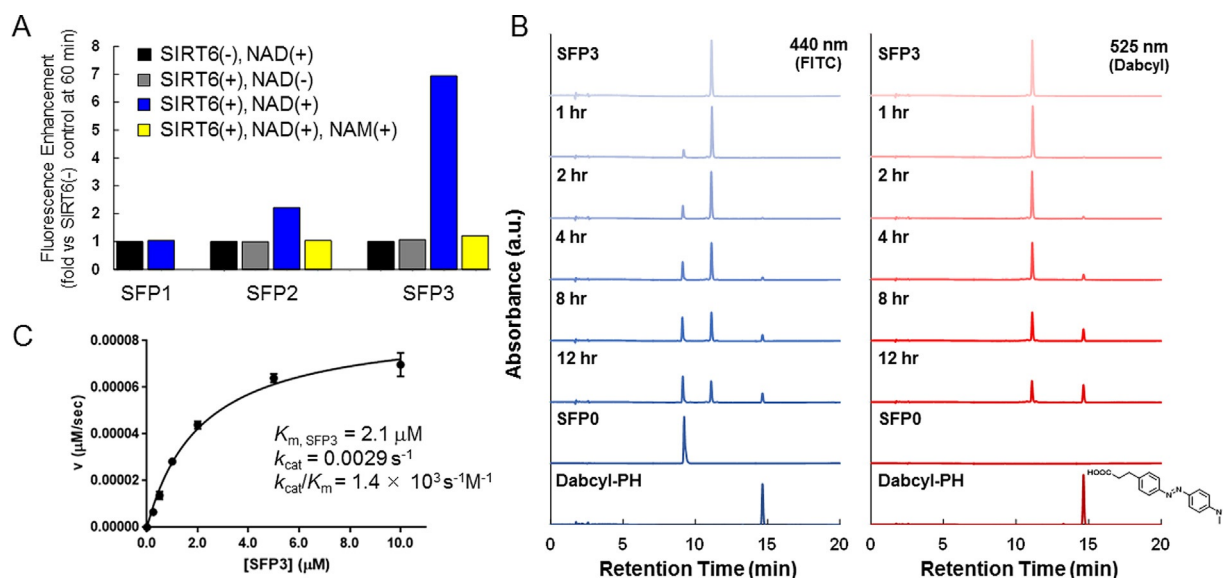


Figure 2. Enzymatic reactions between SFP1–3 and SIRT6. A) Fluorescence enhancement due to enzymatic reactions between SFP1–3 and SIRT6. Reactions were performed with 2.5 μM SFP1–3, 48 nM SIRT6, and 500 μM NAD in SIRT assay buffer [50 mM Tris-HCl (pH 8.0) containing 150 mM NaCl and 1 mM dithiothreitol] at 37 °C. NAM (5 mM) was used as a pan-SIRT inhibitor. $\lambda_{\text{ex}} = 490$ nm, $\lambda_{\text{em}} = 520$ nm. B) HPLC analyses of enzymatic reactions of 20 μM SFP3 and 500 μM NAD with 300 nM SIRT6. Absorbances at 440 and 525 nm, which are the absorbance maxima of FITC and Dabcy, respectively, under acidic conditions were monitored. C) Michaelis–Menten plot of SFP3 reaction with SIRT6. The K_{m} value is calculated to be 2.1 μM .

Activities of other SIRT family members towards SFP3

It has been reported that SIRT1–3 showed strong demyristoylase activity, whereas SIRT4 did not.^[13] We found that the reaction between SFP3 and SIRT1 proceeded even more rapidly than that between SFP3 and SIRT6 (Figure 3A). Kinetic analysis revealed that SFP3 is an excellent substrate of SIRT1: the K_m and k_{cat} values were calculated to be $0.10 \mu\text{M}$ and $0.023 \text{ s}^{-1} \text{ M}^{-1}$, respectively (Table 2, Figure S2). SFP3 was also moderately susceptible to SIRT2 and SIRT3, but was not hydrolyzed by SIRT4 (Figure 3B–D). Product analysis of the enzymatic reaction between SFP3 and SIRT1 by HPLC showed that SFP0 and DabcyI-PH were generated, without any apparent side reaction (Figure S3). These results again strongly support our idea that the DabcyI-PH group is recognized as efficiently

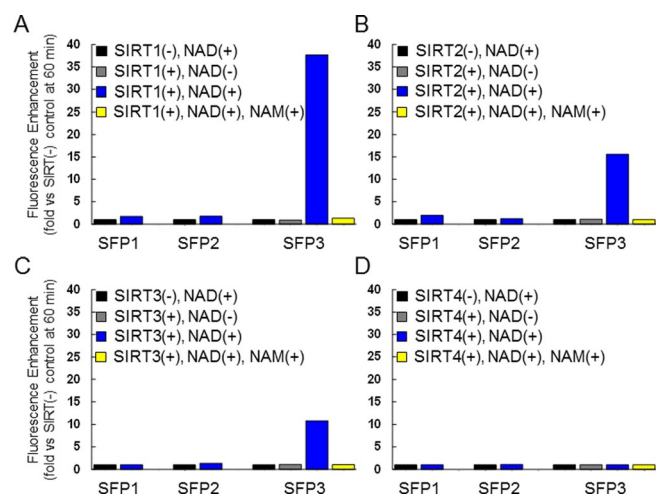


Figure 3. Fluorescence enhancement due to enzymatic reactions between SFP1–3 and SIRTs at 60 min. Reactions were performed with $2.5 \mu\text{M}$ SFP1–3, $500 \mu\text{M}$ NAD, and A) 24 nM SIRT1, B) 48 nM SIRT2, C) 60 nM SIRT3, or D) 32 nM SIRT4, in SIRT assay buffer at 37°C . NAM (5 mM) was used as a pan-SIRT inhibitor. $\lambda_{ex} = 490 \text{ nm}$, $\lambda_{em} = 520 \text{ nm}$.

as myristoyl and palmitoyl groups by various SIRT enzymes. The reactivity (k_{cat}/K_m) of SIRT family members towards SFP3 was as follows: $\text{SIRT1} \gg \text{SIRT2} > \text{SIRT6} > \text{SIRT3} \gg \text{SIRT4}$ (Table 2, Figure S2).

Evaluation of reported SIRT inhibitors and activators with SFP3

We next examined the effects of several SIRT modulators on the hydrolysis of SFP3, because SFP3 detects deacylase activities for long-chain fatty acyl groups, not deacetylase activity, whereas reported SIRT modulators have been identified in terms of action on the deacetylase activity. We focused on NAM and EX-527 as SIRT inhibitors,^[18] and on resveratrol and quercetin as SIRT activators (Figure 4).^[19] EX-527 inhibited SIRT1 ten times more potently than it did SIRT6, which was only weakly inhibited (Figure 4A).^[20] NAM inhibited all the SIRT subtypes tested, with IC_{50} values ranging from 5.6 to $120 \mu\text{M}$ (Figure 4B), in accordance with a previous report.^[21] Resveratrol did not affect SIRT1 activity, but weakly inhibited SIRT6 ($\text{IC}_{50} \approx 190 \mu\text{M}$, Figure 4C). The inhibitory activity of resveratrol towards SIRT1 remains controversial,^[22] and we can at least say that resveratrol did not greatly affect SIRT activity in our assay system. Quercetin had similar effects on SIRT1 and SIRT6 activities: that is, inhibition at lower concentration, but activation at higher concentration, in accordance with a previous report (Figure 4D).^[23] Taken together, these results suggest that SIRT modulators generally have similar effects on deacetylase activity and deacylase activity towards long-chain fatty acyl groups.

Applicability for cell-based assay

Only a little work has been done to evaluate endogenous SIRT activity in living cells.^[24] Therefore, we were interested in applying SFP3 for this purpose. There were two important points to consider: 1) intracellular endopeptidases can hydrolyze SFP3,

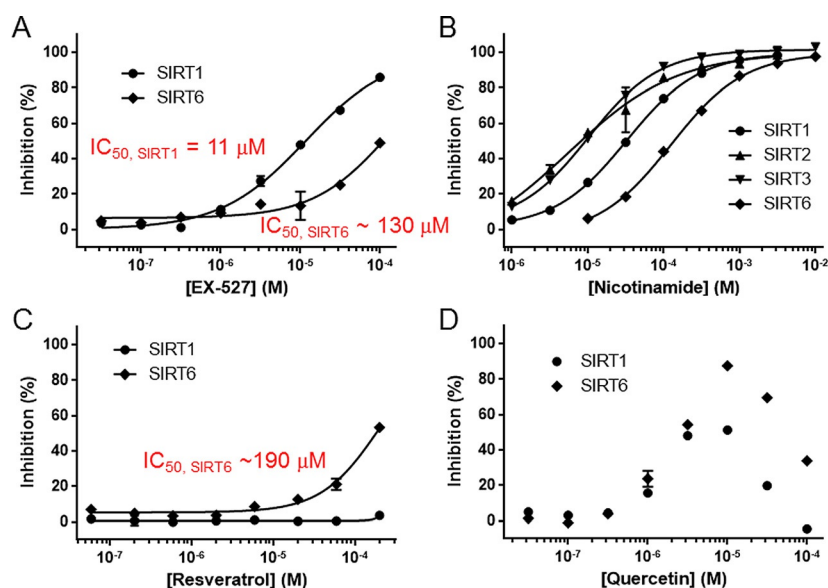


Figure 4. Evaluation of reported SIRT modulators: A) EX-527, B) NAM, C) resveratrol, D) quercetin. IC_{50} values are shown. The results are means \pm SDs ($n = 3$).

and 2) SFP3 might be membrane impermeable because it is a fairly large peptide. To address these points, we first prepared lysates of human embryonic kidney (HEK) 293, HCT116, and PC-3 cells and evaluated the stability of SFP3 in these lysates (Figure S4A). Fluorescence increments were observed in all three lysates, but they were not suppressed in the presence of NAM; this suggested that they were not due to SIRT activity, and that SFP3 was not stable in cell lysates. This was confirmed by HPLC analysis, which indicated that SFP3 afforded complex products in cell lysates, and that these did not include SFP0 or DabcyL-PH (Figure S4B). Thus, SFP3 itself is not applicable to cellular systems.

Modification of SFP3 for intracellular application

We considered that short peptides, up to tripeptides, might be resistant to endopeptidases and might also be more membrane permeable. Therefore, we designed and synthesized four truncated SIRT activity probes: K-F, KS-F, KST-F, and TKT-F, each consisting of a lysine residue bearing DabcyL-PH on the ϵ -amino group as a SIRT deacylation site and linked to one, two, or no other amino acids, on the basis of a previously reported acetylole analysis (Figure 5A, Scheme S5–7).^[25] We measured the absorption and fluorescence spectra of these four probes and calculated the fluorescence quantum yields. All four probes were efficiently quenched by FRET ($\Phi_{FL} = 0.006–0.015$; Figure S5, Table S2). Next, we evaluated the stabilities of these probes in HCT116 cell lysate (Figure 5B). All four probes were much more stable than SFP3 in the lysate. In that experiment, weak fluorescence increments were observed, especially in the

cases of KS-F, KST-F, and TKT-F, and they were suppressed in the presence of NAM, thus suggesting that SIRT activities in the lysate could be detectable by some of these probes. Similar results were obtained with HEK293 and PC-3 cell lysates (Figure S6). We further confirmed that KST-F remained stable in the lysates for at least two hours by means of HPLC analyses (Figure 5C).

We next compared the enzymatic reactions of these probes and SFP3 with SIRT1 (Figure 5D). KS-F, KST-F, and TKT-F showed moderate reactivities with SIRT1 (Figure S7), but K-F showed low reactivity; nevertheless, K-F did react to some degree with SIRT1, and this suggested that even one lysine residue bearing a DabcyL-PH group can be recognized by SIRT1. Kinetic analyses showed that the k_{cat}/K_m values of KS-F, KST-F, and TKT-F were about ten times lower, and that of K-F was 500 times lower, than that of SFP3, thus suggesting that truncating the molecule has little influence on the reactivity with SIRT1 until K-F is reached (Table 3). On the other hand,

Table 3. Kinetic parameters of enzymatic reactions between truncated forms of SFP3 and SIRT1.^[a]

SIRT1	k_{cat} [s^{-1}]	K_m [μM]	k_{cat}/K_m [$s^{-1} M^{-1}$]	$K_{m,NAD}$ [μM]
K-F	0.0021 ± 0.00016	4.6 ± 0.74	4.6×10^2	76
KS-F	0.0055 ± 0.00005	0.39 ± 0.037	1.4×10^4	17
KST-F	0.0063 ± 0.00008	0.38 ± 0.014	1.7×10^4	23
TKT-F	0.0067 ± 0.00002	0.14 ± 0.018	4.8×10^4	4.2

[a] For the determination of kinetic parameters, 7 nM SIRT1 was used. See the Supporting Information for details.

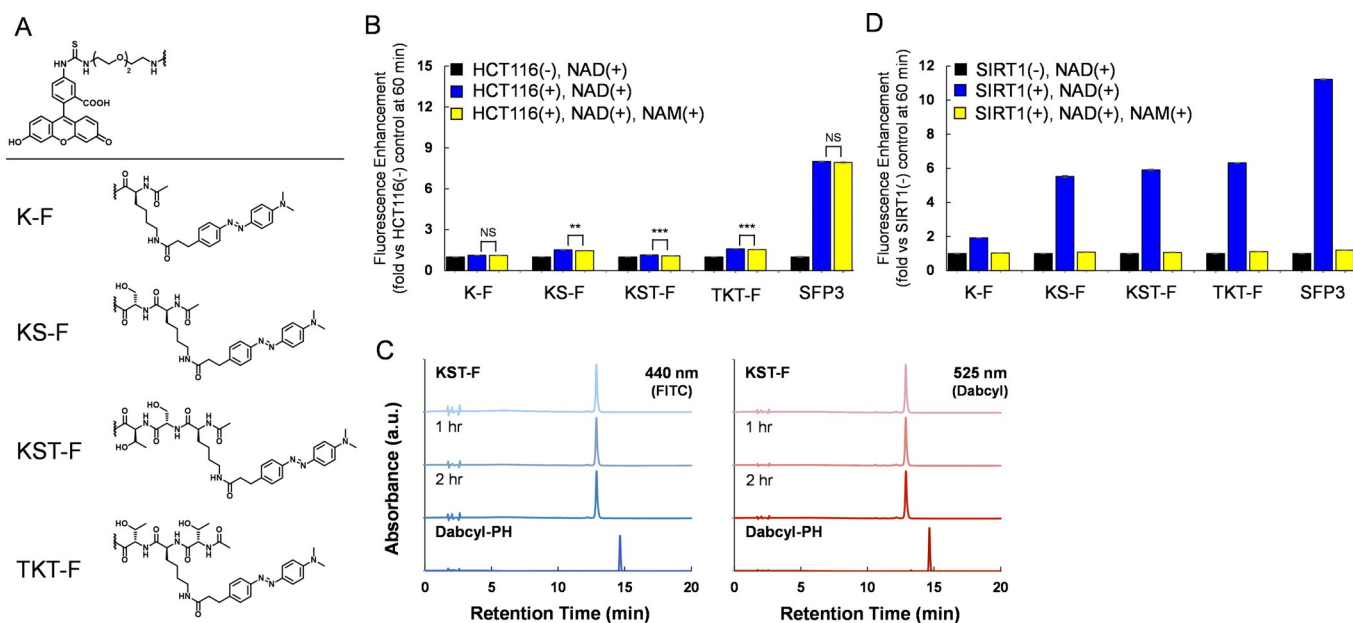


Figure 5. Development of stable, membrane-permeable SIRT probes applicable to cellular systems. A) Structures of the probes. B) Stability of the four SIRT probes and of SFP3 in HCT116 lysate. Reactions were performed with 2.5 μM SIRT probes, 500 μM NAD, and HCT116 lysates (0.4 mg mL⁻¹ protein) in SIRT HTS assay buffer at 37 °C on a microplate. NAM (5 mM) was used as a pan-SIRT inhibitor. C) HPLC analyses of reaction products of 20 μM KST-F in HCT116 cell lysate (0.4 mg mL⁻¹ protein). Absorbances at 440 nm and 525 nm were monitored. D) Fluorescence enhancement due to enzymatic reactions between the probes and SIRT1 at 60 min. Reactions were performed with 2.5 μM SIRT probes, 500 μM NAD, and 20 nM SIRT1 in SIRT HTS assay buffer at 37 °C on a microplate. The results are means \pm SDs ($n = 3$). Asterisks show statistical significances examined by Bonferroni-type multiple t -test: ** $p < 0.01$, *** $p < 0.001$.

the reactivities of the four probes with SIRT2 and -3 were quite low (Figure S8).

Imaging endogenous SIRT1 activity

We considered that KST-F might be practical for imaging SIRT1 activity in cellular systems, due to its stability and low molecular weight. We therefore adopted a well-established strategy for intracellular probes, and prepared a diacetylated derivative of KST-F: KST-F-DA, which would be expected to show high membrane permeability and to be hydrolyzed to KST-F by intracellular esterases. Incubation of KST-F-DA with HEK293 cells resulted in a gradual increase in fluorescence, and pretreatment with 10 mM NAM or 20 μ M EX-527 blocked this increase (Figure 6A, B, D, and E). In contrast, pretreatment with 10 μ M AGK2, a SIRT2-specific inhibitor, did not affect the fluorescence increment (Figure 6B and E), thus supporting the involvement of endogenous SIRT1 activity in generating the fluorescence. In addition, interestingly, stimuli of serum starvation made a fluorescence increment more potent in HEK293 cells (Figure 6C and F), probably due to the activation of sirtuin activity. It has been reported that SIRT1 protein levels were elevated under serum starvation in HEK293 cells, strongly supporting our data.^[26] Because KST-F mainly reacted with SIRT1 *in vitro* (Figures 5D and S7), we consider that the fluorescence increment

is likely predominantly to reflect cytoplasmic and nucleic SIRT1 activities in the cells.

Conclusion

On the basis of recently reported SIRT substrate specificities,^[11,12] we designed and synthesized the FRET-based SIRT probes SFP1–3, each consisting of a nonapeptide derived from histone H3K9 and bearing a Dabcyl quencher dye on the ϵ -amino group of the lysine residue, together with a C-terminal fluorophore. SFP3 showed single-step fluorescence activation due to cleavage of the Dabcyl moiety by SIRT1, -2, -3, and -6. Then, to obtain dyes suitable for intracellular imaging, we set out to improve the stability and membrane permeability by truncating the SFP3 molecule. This strategy proved successful, and one of the resulting probes, KST-F, could visualize endogenous SIRT1 activity in living cells for the first time. We expect our probe to be a useful tool for sophisticated functional studies of native SIRT1.

Experimental Section

¹H NMR spectra were recorded with a JEOL JNM-LA500 or JEOL JNM-A500 spectrometer in the indicated solvent. Chemical shifts (δ) are reported in parts per million relative to the internal standard, tetramethylsilane (TMS). Electrospray ionization (ESI) mass

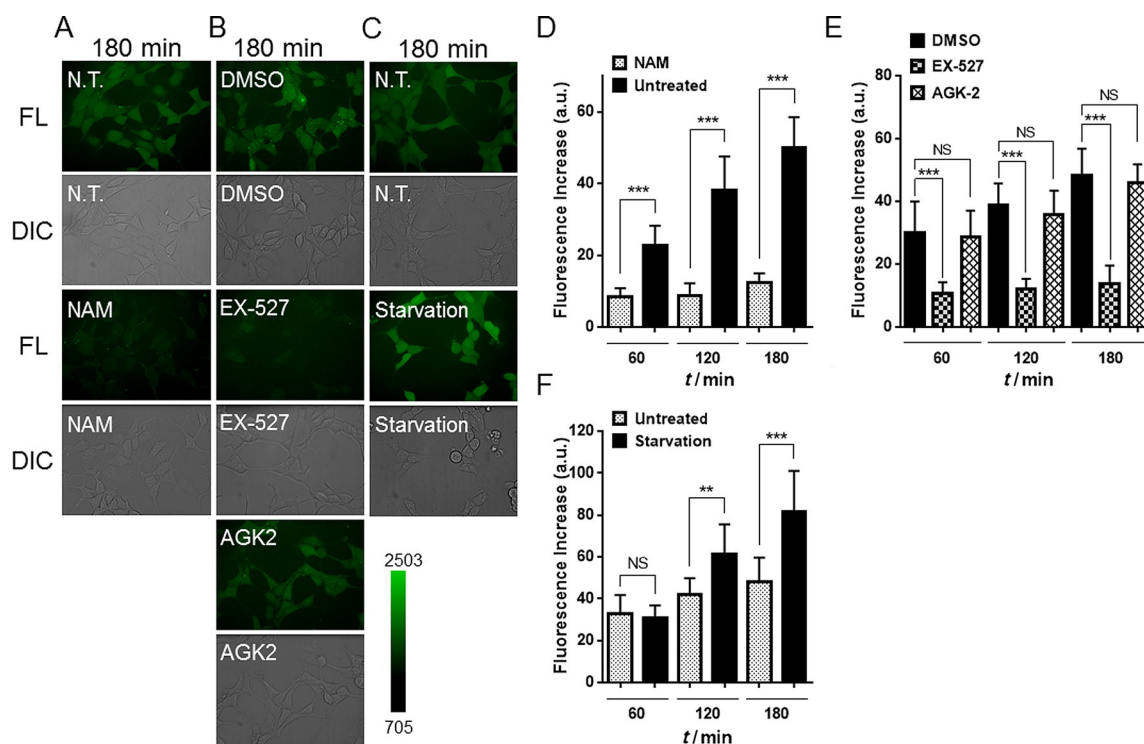


Figure 6. Fluorescence microscopic imaging of SIRT1 activity in living cells with KST-F-DA. HEK293 cells were incubated with 5 μ M KST-F-DA in DPBS in the presence or absence of A) 10 mM NAM, and B) 20 μ M EX-527 (a specific SIRT1 inhibitor) or 10 μ M AGK2 (a specific SIRT2 inhibitor), at 37 °C. C) HEK293 cells were serum starved for 36 h, then incubated with 5 μ M KST-F-DA in DPBS at 37 °C. Confocal fluorescence and differential interference contrast (DIC) images were shown at 180 min after addition of KST-F-DA. D)–F) Comparison of fluorescence intensities of cells treated with DMSO, NAM, EX-527, or AGK2 or serum starved. Fluorescence intensities of regions of interest (inside cells) for each set of conditions were calculated with ImageJ. The results are means \pm SDs ($n = 10$). Asterisks show statistical significances examined by Bonferroni-type multiple t -test: ** $p < 0.01$, *** $p < 0.001$.

spectra were recorded with a JEOL JMS-T100LC mass spectrometer equipped with a nanospray ion source. UV/Vis absorption spectra were recorded with a UV-1800 spectrophotometer. Fluorescence spectra were recorded with an RF-5300PC fluorimeter. Analytical HPLC was performed with a Shimadzu pump system equipped with a reversed-phase ODS column (Inertsil ODS-3 4.6×150 mm, GL Science) at a flow rate of 1.0 mL min⁻¹. Semipreparative HPLC purification was performed with a JASCO PU-2086 pump system equipped with a reversed-phase ODS column (Inertsil ODS-3 20×250 mm, GL Science) at a flow rate of 10 mL min⁻¹. Microplate fluorescence assay was performed with an ARVO X5 platereader (PerkinElmer). Confocal fluorescence images were taken with an IX-71 (Olympus) equipped with disc scanning unit. Recombinant human SIRT1 was purchased from R&D Systems, SIRT2 and SIRT3 were purchased from ATGen, and SIRT4 and SIRT6 were purchased from Bio-Vision. Amino acids and resin were purchased from Watanabe Chemical Industries, Ltd. All other reagents and solvents were purchased from Sigma-Aldrich, Tokyo Chemical Industry Co., Ltd. (TCI), Wako Pure Chemical Industries, Nacalai Tesque, or Kanto Kagaku and used without further purification. Flash column chromatography was performed with silica gel 60 (particle size 0.032–0.075) supplied by Taikoh-shoji.

Acknowledgements

We thank all the members of the H.N. Laboratory. This work was supported in part by JSPS KAKENHI grants no. 15K18899 (M.K.) and 25293028 (H.N.), as well as by the Hori Sciences and Arts Foundation (M.K.), a Grant-in-Aid for Scientific Research on Innovative Areas from MEXT (26111012, H.N.) and a grant from the Daiichi Sankyo Foundation of Life Science (H.N.), and the Platform Project for Supporting in Drug Discovery and Life Science Research (Platform for Drug Discovery, Informatics, and Structural Life Science) from the Japan Agency for Medical Research and Development (AMED).

Keywords: enzymatic reaction · fluorescent probes · FRET · imaging agents · quencher dyes · sirtuins

- [1] a) S. Imai, C. M. Armstrong, M. Kaeberlein, L. Guarente, *Nature* **2000**, *403*, 795–800; b) R. H. Houtkooper, E. Pirinen, J. Auwerx, *Nat. Rev. Mol. Cell Biol.* **2012**, *13*, 225–238.
- [2] a) M. C. Haigis, L. P. Guarente, *Genes Dev.* **2006**, *20*, 2913–2921; b) V. D. Longo, B. K. Kennedy, *Cell* **2006**, *126*, 257–268; c) A. A. Sauve, C. Wolberger, V. L. Schramm, J. D. Boeke, *Annu. Rev. Biochem.* **2006**, *75*, 435–465; d) T. Finkel, C. X. Deng, R. Mostoslavsky, *Nature* **2009**, *460*, 587–591.
- [3] a) S. Lavu, O. Boss, P. J. Elliott, P. D. Lambert, *Nat. Rev. Drug Discovery* **2008**, *7*, 841–853; b) J. C. Milne, P. D. Lambert, S. Schenk, D. P. Carney, J. J. Smith, D. J. Gagne, L. Jin, O. Boss, R. B. Perni, C. B. Vu, J. E. Bemis, R. Xie, J. S. Disch, P. Y. Ng, J. J. Nunes, A. V. Lynch, H. Yang, H. Galonek, K. Israelian, W. Choy, A. Iffland, S. Lavu, O. Medvedik, D. A. Sinclair, J. M. Olefsky, M. R. Jirousek, P. J. Elliott, C. H. Westphal, *Nature* **2007**, *450*, 712–716; c) L. Guarente, *N. Engl. J. Med.* **2011**, *364*, 2235–2244; d) J. Hu, H. Jing, H. Lin, *Future Med. Chem.* **2014**, *6*, 945–966.
- [4] D. Kölle, G. Brosch, T. Lechner, A. Lusser, P. Loidl, *Methods* **1998**, *15*, 323–331.
- [5] D. Herman, K. Jenssen, R. Burnett, E. Soragni, S. L. Perlman, J. M. Gottesfeld, *Nat. Chem. Biol.* **2006**, *2*, 551–558.
- [6] B. C. R. Dancy, S. A. Ming, R. Papazyan, C. A. Jelinek, A. Majumgar, Y. Sun, B. M. Dancy, W. J. Drury III, R. J. Cotter, S. D. Taverna, P. A. Cole, *J. Am. Chem. Soc.* **2012**, *134*, 5138–5148.
- [7] a) M. T. Borra, B. C. Smith, J. M. Denu, *J. Biol. Chem.* **2005**, *280*, 17187–17195; b) Y. Li, T. Liu, S. Liao, Y. Li, Y. Lan, A. Wang, Y. Wang, B. He, *Biochem. Biophys. Res. Commun.* **2015**, *467*, 459–466.
- [8] a) R. Baba, Y. Hori, S. Mizukami, K. Kikuchi, *J. Am. Chem. Soc.* **2012**, *134*, 14310–14313; b) R. Baba, Y. Hori, K. Kikuchi, *Chemistry* **2015**, *21*, 4695–4702.
- [9] J. C. Tanny, G. J. Dowd, J. Huang, H. Hilz, D. Moazed, *Cell* **1999**, *99*, 735–745.
- [10] R. A. Mathias, T. M. Greco, A. Oberstein, H. G. Budayeva, R. Chakrabarti, E. A. Rowland, Y. Kang, T. Shenk, I. M. Cristea, *Cell* **2014**, *159*, 1615–1625.
- [11] J. Du, Y. Zhou, X. Su, J. J. Yu, S. Khan, H. Jiang, J. Kim, J. Woo, J. H. Kim, B. H. Choi, B. He, W. Chen, S. Zhang, R. A. Cerione, J. Auwerx, Q. Hao, H. Lin, *Science* **2011**, *334*, 806–809.
- [12] H. Jiang, S. Khan, Y. Wang, G. Charron, B. He, C. Sebastian, J. Du, R. Kim, E. Ge, R. Mostoslavsky, H. C. Hang, Q. Hao, H. Lin, *Nature* **2013**, *496*, 110–113.
- [13] J. L. Feldman, J. Baeza, J. M. Denu, *J. Biol. Chem.* **2013**, *288*, 31350–31356.
- [14] Y. B. Teng, H. Jing, P. Aramsangtienchai, B. He, S. Khan, J. Hu, H. Lin, Q. Hao, *Sci. Rep.* **2015**, *5*, 8529.
- [15] S. Schuster, C. Roessler, M. Meleshin, P. Zimmermann, Z. Simic, C. Kambach, C. Schiene-Fischer, C. Steegborn, M. O. Hottiger, M. Schutkowski, *Sci. Rep.* **2016**, *6*, 22643.
- [16] E. Michishita, R. A. McCord, E. Berber, M. Kioi, H. Padilla-Nash, M. Damian, P. Cheung, R. Kusumoto, T. L. Kawahara, J. C. Barrett, H. Y. Chang, V. A. Bohr, T. Ried, O. Gozani, K. F. Chua, *Nature* **2008**, *452*, 492–496.
- [17] M. T. Borra, M. R. Langer, J. T. Slama, J. M. Denu, *Biochemistry* **2004**, *43*, 9877–9887.
- [18] a) A. D. Napper, J. Hixon, T. McDonagh, K. Keavey, J. F. Pons, J. Barker, W. T. Yau, P. Amouzegh, A. Flegg, E. Hamelin, R. J. Thomas, M. Kates, S. Jones, M. A. Navia, J. O. Saunders, P. S. DiStefano, R. Curtis, *J. Med. Chem.* **2005**, *48*, 8045–8054; b) M. Gertz, F. Fischer, G. T. Nguyen, M. Lakshminarasimhan, M. Schutkowski, M. Weyand, C. Steegborn, *Proc. Natl. Acad. Sci. USA* **2013**, *110*, E2772–2781.
- [19] K. T. Howitz, K. J. Bitterman, H. Y. Cohen, D. W. Lamming, S. Lavu, J. G. Wood, R. E. Zipkin, P. Chung, A. Kisielewski, L. L. Zhang, B. Scherer, D. A. Sinclair, *Nature* **2003**, *425*, 191–196.
- [20] P. Kokkonen, M. Rahnasto-Rilla, P. Mellini, E. Jarho, M. Lahtela-Kakkonen, T. Kokkola, *Eur. J. Pharm. Sci.* **2014**, *63*, 71–76.
- [21] J. L. Feldman, K. E. Dittenhafer-Reed, N. Kudo, J. N. Thelen, A. Ito, M. Yoshida, J. M. Denu, *Biochemistry* **2015**, *54*, 3037–3050.
- [22] S. J. Park, F. Ahmad, A. Philp, K. Baar, T. Williams, H. Luo, H. Ke, H. Rehmann, R. Taussig, A. L. Brown, M. K. Kim, M. A. Beaven, A. B. Burgin, V. Manganiello, J. H. Chung, *Cell* **2012**, *148*, 421–433.
- [23] M. Rahnasto-Rilla, T. Kokkola, E. Jarho, M. Lahtela-Kakkonen, R. Moaddel, *Chembiochem* **2016**, *17*, 77–81.
- [24] Y. Wang, Y. Chen, H. Wang, Y. Cheng, X. Zhao, *Anal. Chem.* **2015**, *87*, 5046–5049.
- [25] D. Rauh, F. Fischer, M. Gertz, M. Lakshminarasimhan, T. Bergbrede, F. Aladini, C. Kambach, C. F. Becker, J. Zerweck, M. Schutkowski, C. Steegborn, *Nat. Commun.* **2013**, *4*, 2327.
- [26] Y. Kanfi, V. Peshti, Y. M. Gozlan, M. Rathaus, R. Gil, H. Y. Cohen, *FEBS Lett.* **2008**, *582*, 2417–2423.

Manuscript received: July 3, 2016

Accepted article published: August 19, 2016

Final article published: September 9, 2016